

INVITED REVIEW PAPER

## Organic solar cells based on conjugated polymers : History and recent advances

Hwajeong Kim<sup>\*</sup>, Sungho Nam<sup>\*</sup>, Jaehoon Jeong<sup>\*</sup>, Sooyong Lee, Jooyeok Seo, Hyemi Han, and Youngkyoo Kim<sup>†</sup>

Organic Nanoelectronics Laboratory, Department of Chemical Engineering, School of Applied Chemical Engineering, Kyungpook National University, Daegu 702-701, Korea  
(Received 26 January 2014 • accepted 2 June 2014)

**Abstract**—Organic solar cells have attracted huge attention because of their potential in the low-cost manufacturing of plastic solar modules featuring flexible, lightweight, ultrathin, rollable and bendable shapes. The power conversion efficiency of organic solar cells is now passing ~10%, which is a critical sign toward commercialization because organic solar cells surpass any other types of solar cells in terms of development speed. The encouraging efficiency enhancement could be realized by introducing a ‘bulk heterojunction’ concept that overcomes the weakness of organic semiconductors by minimizing their charge transport paths through making effective p-n junctions inside bulk organic films. However, there are several hurdles for commercialization, including stability and lifetime issues, owing to the bulk heterojunction concept. This review summarizes the important aspects of organic solar cells, particularly focusing on conjugated polymers as an active layer component.

**Keywords:** Organic Solar Cells, Power Conversion Efficiency, Bulk Heterojunction, Conjugated Polymer, Flexible, Charge Transport

### INTRODUCTION

Solar cells, without any doubt, have been recognized as one of the important energy conversion devices that can directly deliver electricity from sun light. As far as the sun light shines to our planet, the electricity production via solar cells is expected endlessly without any payment for using the sun light. However, we understand very well that the electricity from solar cells is more expensive than conventional electricity from fossil fuel and/or nuclear power stations [1,2]. The reason is related to the high manufacturing cost for conventional solar cells, which are mostly based on inorganic materials and need high temperature processes and expensive vacuum systems [3-5].

### BIRTH OF ORGANIC SOLAR CELLS

To overcome the cost issue in conventional solar cells, organic materials have been introduced as a light absorption material from 1906 to 1995 (see Table 1) because of their potential for low temperature and/or vacuum-free processes [6-20]. Of these early studies, three pioneering works can be highlighted when it comes to the practical applications to date. The first pioneering work can be attributed to the fabrication of bilayer-type organic solar cells using small molecules [15]. The bilayer-type organic solar cells showed a striking efficiency jump up to ~0.9%, which had never been expected for organic materials at that time. However, the drawback of this work by Tang was that vacuum systems were still mandatory to deposit organic layers. The second pioneering work can be assigned to the invention of bulk heterojunction structures by mix-

ing soluble conjugated polymers and fullerenes in 1992 [17]. The last pioneering work can go for the realization of bulk heterojunction structures with p-type and n-type polymers in 1995, which was first published by Friend group and then Heeger group [19,20].

Fig. 1 summarizes three representative device structures of organic solar cells and organic materials used for the devices. The single layer structure (Fig. 1(a)) has an intrinsic limitation in achieving high efficiency because the organic layer, where it is p-type or n-type, between electrodes cannot properly generate individual charges (holes and electrons) owing to the extremely low charge separation yield originated from the nature of tightly-bound excitons in organic semiconductors [21,22]. To help the separation of charges from excitons, a bilayer structure has been introduced by stacking p-type and n-type organic layers (Fig. 1(b)). Although the bilayer structure could improve the charge separation at the interfaces between p-type and n-type organic semiconducting layers, a limitation still remains because of poor charge transport inside each organic layer [23,24]. In this regard, the bulk heterojunction (BHJ) structure (Fig. 1(c)) is of crucial importance because it can resolve two intrinsic issues, charge separation and charge transport, in organic layers [17-20]. These three are representative structures; however, they have a fundamental limitation in terms of open circuit voltage ( $V_{oc}$ ) that is basically determined by the offset energy between the highest occupied molecular orbital (HOMO) of p-type organic semiconductors and the lowest unoccupied molecular orbital (LUMO) of n-type organic semiconductors, even though the work functions of electrodes often affect  $V_{oc}$  [25,26]. To maximize the power conversion efficiency in organic solar cells by increasing  $V_{oc}$ , a tandem structure (Fig. 2) can be applied because the overall voltage becomes the sum of individual  $V_{oc}$  values in each sub cell (front and back cells) [27,28]. In addition, the overall short circuit current density ( $J_{sc}$ ) of tandem cells can be enhanced by selecting complementary BHJ layers, which have different absorption ranges for maximizing solar light harvesting, even though an adverse effect is also present owing to marginally increased electri-

<sup>†</sup>To whom correspondence should be addressed.  
E-mail: ykimm@knu.ac.kr

<sup>\*</sup>These authors contributed equally to this work.

Copyright by The Korean Institute of Chemical Engineers.

**Table 1. Summary of key materials/structures used in organic solar cells reported from 1906 to 1995**

Year	First author	Materials/Device structures	PCE (%)	Light intensity	Reference
1906	A. Pochettino	Anthracene crystals	-	-	6
1910	J. Koenigsberger	Benzene derivatives	-	-	7
1953	H. Mette	Antracene	-	-	8
1957	H. Hoegel	Poly(N-vinyl carbazole) (PVK)	-	-	9
1959	H. Kallmann	Anthracene	~0.1%	-	10
1960	O. H. Le Blanc	Anthracene	-	-	11
1960	R. G. Kepler	Anthracene crystals	-	-	12
1962	P. Mark	p-Terphenyl, p-quaterphenyl, anthracene	-	-	13
1966	N. Geacintov	Tetracene-water	-	-	14
1986	C. W. Tang	CuPc/PV	0.95%	75 mW/cm <sup>2</sup>	15
1990	B. A. Gregg	Liquid crystalline porphyrins	$V_{oc} : 0.3 \text{ V}$ $J_{sc} : 0.4 \text{ mA/cm}^2$	100 mW/cm <sup>2</sup>	16
1992	N. S. Sariciftci	MEH-PPV : C <sub>60</sub>			17
1995	G. Yu	MEH-PPV : PC <sub>61</sub> BM	2.9%	20 mW/cm <sup>2</sup> at 430 nm	18

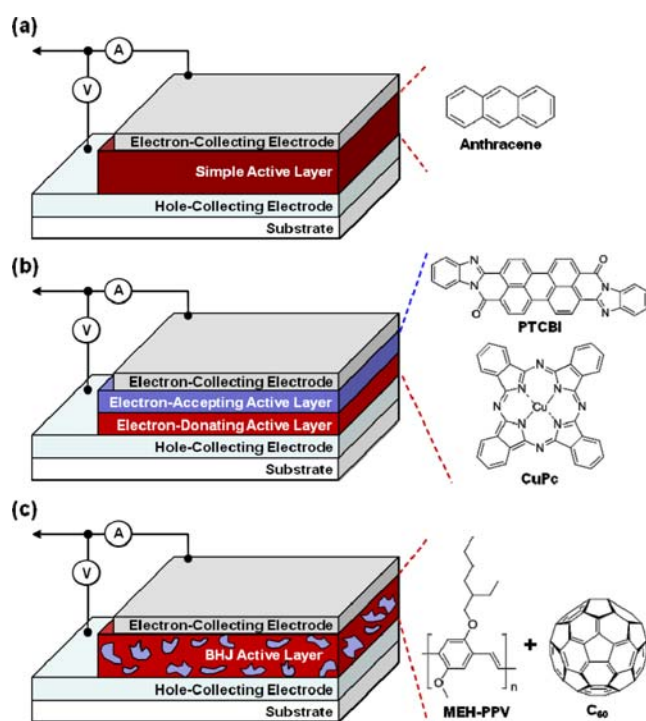


**Fig. 1. Three representative device structures for organic solar cells: (a) single active layer; (b) double active layer (p-n junction bilayer); (c) bulk heterojunction active layer. The chemical structures in each device structure show materials that were first used for corresponding device structures.**

cal resistances by the presence of additional interfaces and active layers in series connection [27,28]. As illustrated in Fig. 2, both normal-type and inverted-type structures are possible by placing suitable electrodes with appropriate work functions on each side.

### BULK HETEROJUNCTION (BHJ) STRUCTURE

As briefly mentioned above, the bulk heterojunction structure (Fig. 1(c)) is one of the most practical structures because of simple

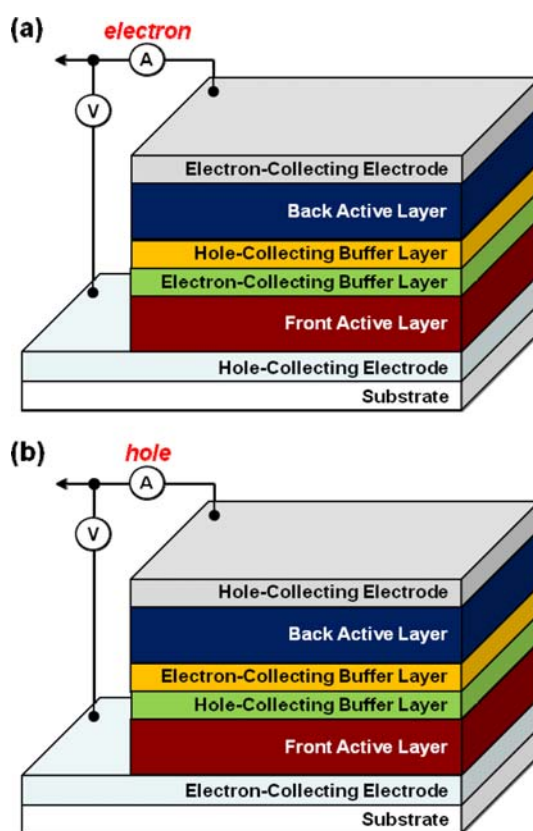


**Fig. 2. Two different structures of tandem organic solar cells: (a) normal-type structure, (b) inverted-type structure.**

fabrication of active layers similar to the single layer structure (see Fig. 1(a)). As illustrated in Fig. 3, excitons are generated at the interfaces between p-type and n-type domains of organic semiconductors inside bulk organic composite (blend) films. Here we note that the number of p-n junction interfaces is expected to reach a theoretical limit, if both p-type and n-type organic semiconductors are mixed on a molecular scale, but it will be far less than the theoretical limit in actual devices. Then the excitons generated at the interfaces undergo charge separation processes, which are enabled by

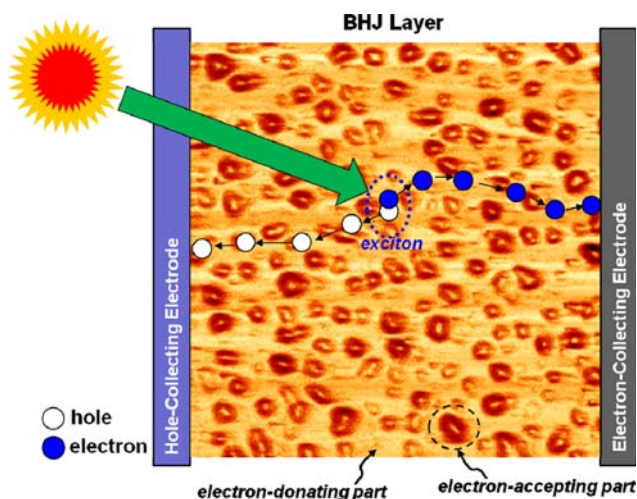


Fig. 3. Illustration for the mechanism (exciton generation, charge separation, charge transport, and charge collection) in organic solar cells with bulk heterojunction active layers. Note that an AFM image (P3HT : PC<sub>61</sub>BM film) was inserted between the hole-collecting electrode and the electron-collecting electrode in order to better explain the mechanism graphically.

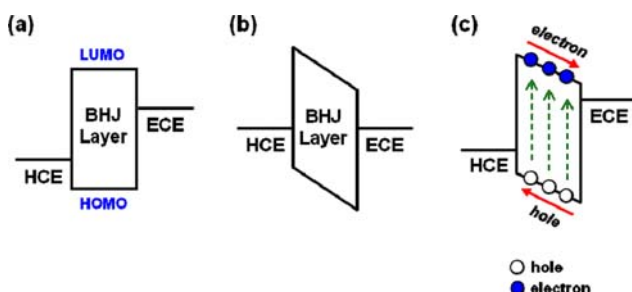


Fig. 4. Change of energy bands in the bulk heterojunction (BHJ) layer between hole-collecting electrode (HCE) and electron-collecting electrode (ECE): (a) no contact (flat energy band), (b) short circuit condition, (c) under light illumination (photovoltaic action).

the HOMO-LUMO offset energy between p-type and n-type organic semiconductors as explained in the above section. This charge separation step produces individual charges, holes and electrons, which transport through neighboring p-type and n-type organic semiconductor domains, respectively, toward corresponding electrodes. As shown in Fig. 4, the transport of holes and electrons to electrodes is mostly driven by the built-in electric field caused by the Fermi level alignment (Fig. 4b)) between the two electrodes in the presence of the active layer. This can be assigned to a drift current associated with the built-in electric field, but a diffusion current is also expected to contribute to the overall current. As depicted in Fig. 4(c), the generated charges give rise to the actual work function difference of electrodes upon illumination, which further increases the built-in electric field leading to better charge transport in actual devices. Note that the charge transport in the bulk heterojunction structures is one of the most important limiting factors because p-type and n-type organic semiconductors are mixed in the active layer.

The fabrication process for a normal-type solar cell with a bulk

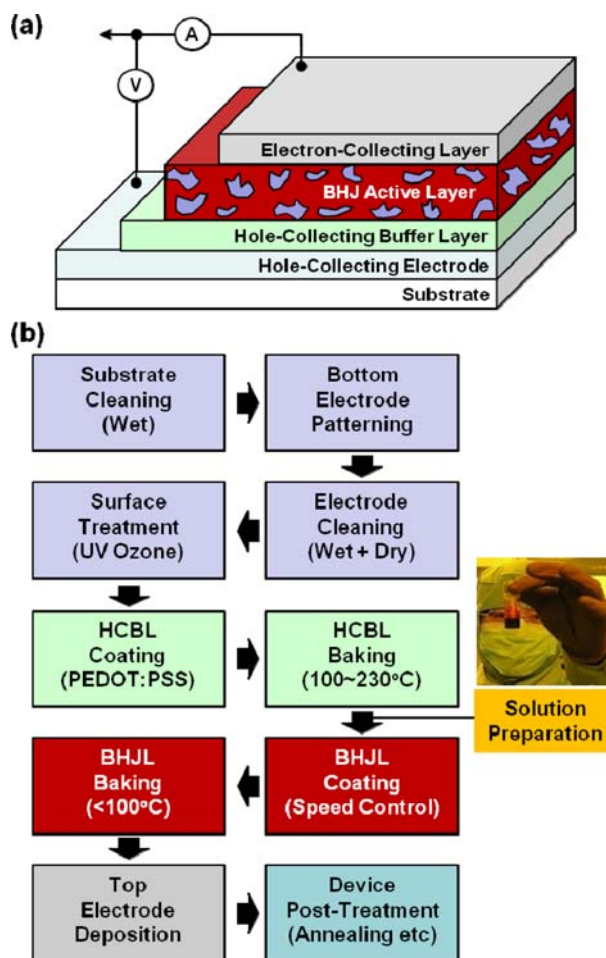


Fig. 5. Device structure (a) and fabrication process (b) for BHJ organic solar cells with a hole-collecting buffer layer.

heterojunction layer is briefly summarized in Fig. 5. The first step is the preparation (cleaning and etching etc.) of substrates, which is of importance because the states of substrate surfaces govern the quality of whole devices. At the same time, solutions of p-type and n-type organic semiconductors (mostly soluble conjugated polymers) should be prepared desirably one day before for optimum mixing between the two materials in the presence of solvents. Next, a hole-collecting buffer layer (HCBL) is coated on the electrodes of substrates, followed by appropriate soft-baking step. The quality of HCBL does greatly affect the performance of organic solar cells because it is closely related with the hole collection efficiency. On top of the hole-collecting buffer layer, the bulk heterojunction layer (BHJL) is coated and soft-baked to remove any possible solvent molecules remained inside the BHJ layer. Finally, a top electrode is deposited on the BHJ layer, which is carried out by thermal evaporation of metals in vacuum and/or by wet-coating using metallic inks [29,30]. The completed devices can be finally subject to post-treatment processes according to the nature of organic semiconductors. For example, the bulk heterojunction layers containing regioregular poly(3-hexylthiophene) (P3HT) should undergo thermal annealing processes to induce recrystallization of P3HT chains [31-36]. However, a thermal annealing deteriorates the performance of organic solar cells with a bulk heterojunction layer containing poly[2-



methoxy-5-(3,7'-dimethyloctyloxy)-1,4-phenylenevinylene] (MDMO-PPV) or poly[[4,8-bis[(2-ethylhexyl)oxy]benzo[1,2-b:4,5-b']dithiophene-2,6-diyl][3-fluoro-2-[(2-ethylhexyl)carbonyl]thieno[3,4-b]thiophenediyl]] (PTB7) [37-41].

### POLYMER : FULLERENE SOLAR CELLS

To date, the most popular bulk heterojunction structure is made with the composites of conjugated polymers (p-type) and fullerene derivatives (n-type), leading to polymer : fullerene solar cells. Since early conceptual works [17,18], a significant breakthrough was made by Shaheen et al. for polymer : fullerene solar cells through the nanomorphology control of bulk heterojunction films [37]. They simply changed solvent from toluene to chlorobenzene in order to dissolve MDMO-PPV and [6,6]-phenyl-C<sub>61</sub>-butyric acid methyl ester (PC<sub>61</sub>BM), which delivered a finer film morphology (MDMO-PPV : PC<sub>61</sub>BM = 1 : 4 by weight) leading to greatly enhanced short circuit current density ( $J_{sc}$ ) from 2.33 mA/cm<sup>2</sup> to 5.25 mA/cm<sup>2</sup>. The fill factor (FF) was also increased from 50% to 61%, which resulted in the PCE improvement from 0.9% to 2.5% [37,38]. As shown in

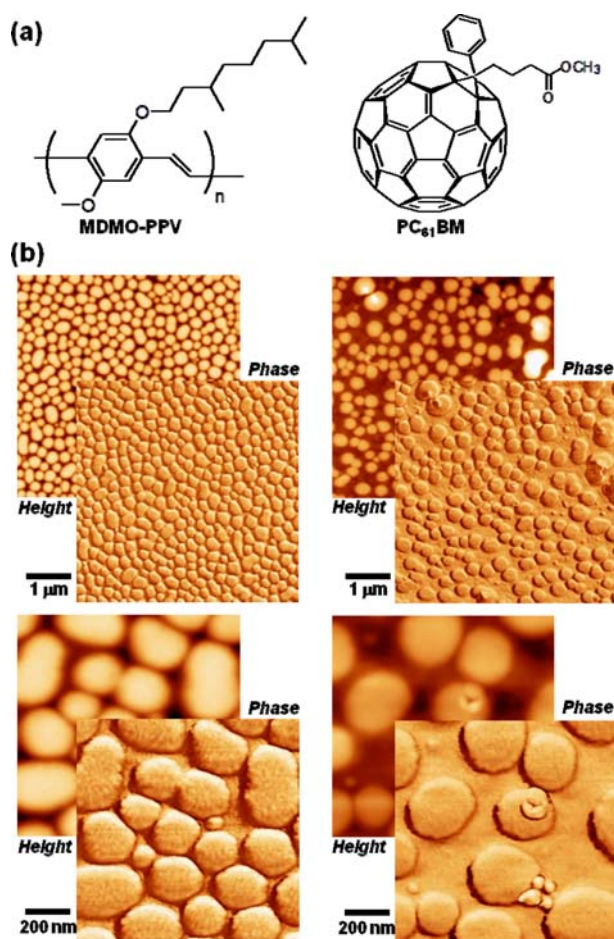


Fig. 6. (a) Chemical structure of MDMO-PPV and PC<sub>61</sub>BM. (b) AFM images (height and phase modes) of MDMO-PPV : PC<sub>61</sub>BM bulk heterojunction films prepared using chlorobenzene (left) and toluene (right): Note that individual scans were applied for each image (top: 5 μm × 5 μm, bottom: 1 μm × 1 μm).

Fig. 6, our own measurement showed that the morphology of films prepared using chlorobenzene and toluene was different from each other in terms of fullerene domain enrichment on the film surface but the size of phase segregation seemed to be similar. Interestingly, the PCE was rather decreased from 1.23% to 0.49% by annealing the MDMO-PPV : PC<sub>61</sub>BM film (1 : 1 by weight) at 110 °C, which might be too high to make an optimum phase-segregated morphology when it comes to the relatively low glass transition temperature of MDMO-PPV (~80 °C) [42]. This land-mark work initiated tremendous interest and research in polymer : fullerene solar cells. However, the power conversion efficiency of MDMO-PPV : PC<sub>61</sub>BM solar cells has an intrinsic limitation because the optical absorption range of MDMO-PPV is less than 600 nm (wavelength). Hence P3HT polymers have been introduced because they can absorb visible light up to 650 nm and their glass transition temperature approaches ~110 °C [31-36,43-45]. In addition, the external quantum efficiency (EQE) of devices at a maximum wavelength reached more than 70% for P3HT : PC<sub>61</sub>BM solar cells, compared to ~50% for MDMO-PPV : PC<sub>61</sub>BM solar cells (see Fig. 7). Such high EQE for P3HT : PC<sub>61</sub>BM solar cells can be ascribed to the extremely high tendency of chain stacking (recrystallization) in regioregular P3HT films and resulting high charge carrier mobility, which was confirmed from the systematic study on the P3HT regularity effect by Kim et al. [36]. However, the open circuit voltage ( $V_{oc}$ ) of P3HT : PC<sub>61</sub>BM solar cells is relatively lower than that of MDMO-PPV : PC<sub>61</sub>BM solar cells because the HOMO energy level of P3HT (~5.0 eV) is higher than that of MDMO-PPV (~5.3 eV) (see Fig. 8). Thus the practical power conversion efficiency of P3HT : PC<sub>61</sub>BM solar cells was 4-5% when PC<sub>61</sub>BM was used as an electron-acceptor [31-36]. Here we note that the  $V_{oc}$  of P3HT : fullerene solar cells was noticeably increased by introducing bis-adduct fullerene derivatives such as indene-C<sub>60</sub> bis-adduct (ICBA) [46].

To improve the power conversion efficiency of polymer : fullerene solar cells, various conjugated polymers with narrower band gaps

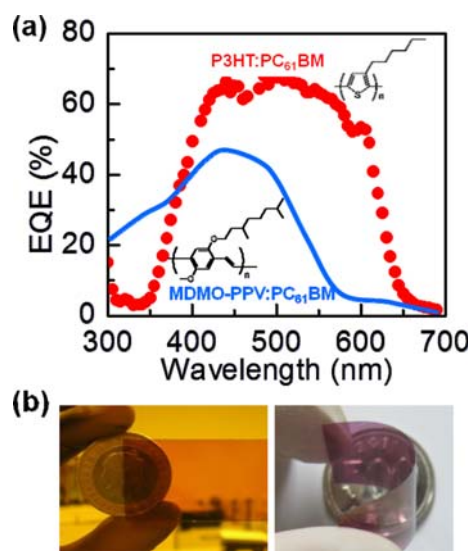


Fig. 7. (a) EQE comparison of organic solar cells with the P3HT : PC<sub>61</sub>BM film and the MDMO-PPV : PC<sub>61</sub>BM film. (b) Photographs of the P3HT : PC<sub>61</sub>BM films coated on a glass substrate (left) and on a flexible plastic substrate (right).

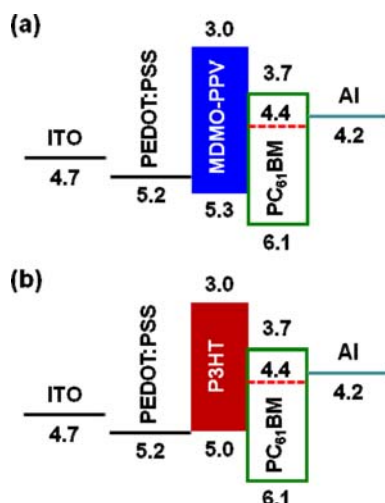


Fig. 8. Flat energy band diagrams for organic solar cells with (a) the MDMO-PPV:PC<sub>61</sub>BM film and (b) the P3HT:PC<sub>61</sub>BM film.

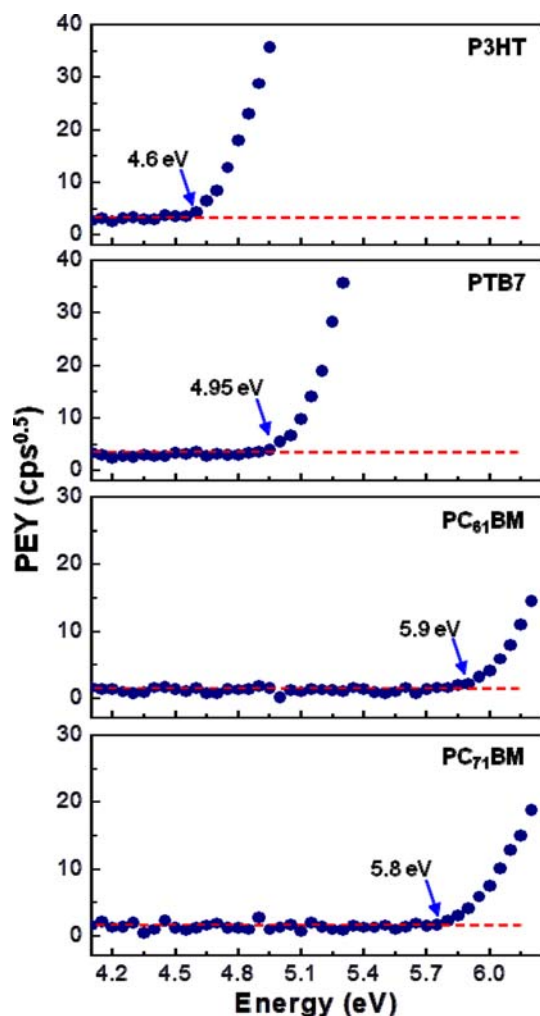


Fig. 9. Photoelectron yield (PEY) spectra for two representative electron-donating polymers (P3HT and PTB7) and two representative electron-accepting fullerenes (PC<sub>61</sub>BM and PC<sub>71</sub>BM). The onset point, which is given on each plot, is subject to calibration to get an accurate HOMO energy level.

(compared to P3HT) have been developed [39-41,47-55]. The optical absorption range of PTB7 reaches ~750 nm, while the HOMO energy level of PTB7 is around -5.2 eV. As shown in Fig. 9, the

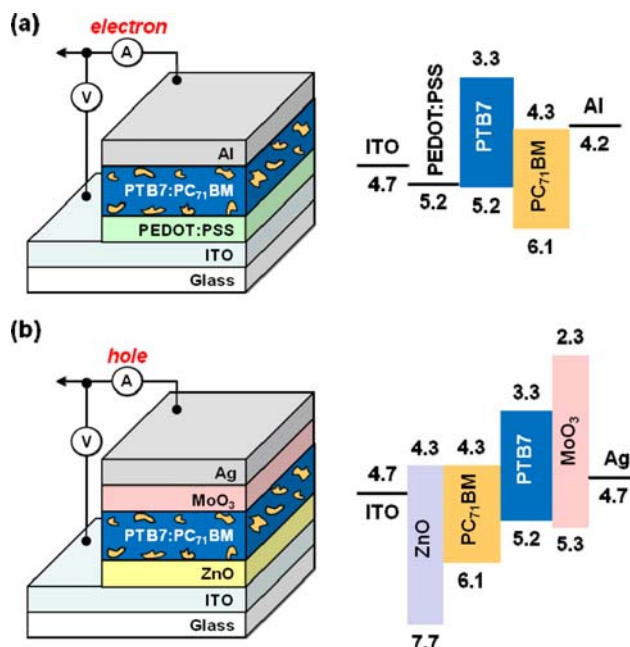


Fig. 10. Device structures (left) and flat energy band diagrams (right) for organic solar cells with the PTB7:PC<sub>71</sub>BM film: (a) normal-type device, (b) inverted-type structure.

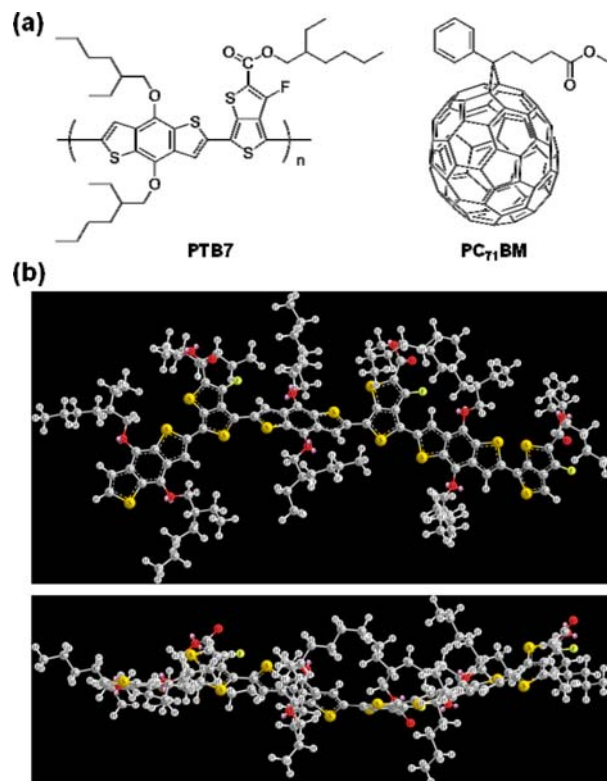


Fig. 11. (a) Chemical structure of PTB7 and PC<sub>71</sub>BM. (b) Energy minimized structures (top view and side view) of three repeating units of PTB7.

ionization potential of PTB7 is relatively higher than that of P3HT. Considering the LUMO energy level of fullerene derivatives in solid-state films ( $-3.7$  eV $\sim$  $-4.4$  eV) [56,57], the  $V_{oc}$  from the solar cells with the bulk heterojunction films of PTB7 and fullerene derivatives is expected to be  $\sim 0.8$  V at least. In accordance with this estimation, the measured  $V_{oc}$  values did fall into  $0.7$ - $0.8$  V [39-41]. To increase the built-in electric field for better charge transport and higher  $V_{oc}$ , various approaches have been attempted to modify the interfaces between active layers and electrodes or buffer layers inside the PTB7 : fullerene solar cells [40,41]. The highest power conversion efficiency of single stacked polymer : fullerene solar cells is so far  $\sim 9.2\%$  using the PTB7 polymer as an electron donor and [6,6]-

phenyl-C<sub>71</sub>-butyric acid methyl ester (PC<sub>71</sub>BM) as an electron acceptor [40,41]. Fig. 10 shows typical device structures of normal-type and inverted-type P3HT : PC<sub>71</sub>BM solar cells. As mentioned, the PTB7 : PC<sub>71</sub>BM solar cells, whether they are normal or inverted structures, can lose high efficiency once a thermal annealing applies. The reason can be found from the molecular structure of PTB7, which is different from that of P3HT [36]. As shown in Fig. 11(a), the PTB7 polymer has asymmetrically-attached alkyl chains in the backbone, which is expected to prevent the PTB7 polymer chains from stacking compactly each other. The random alignment of alkyl chains and resulting backbone distortion can be seen from the energy minimized structures in Fig. 11(b). The best performance of polymer :

**Table 2. Summary of key materials/structures used in organic solar cells with polymer : fullerene bulk heterojunction layers**

Year	First author	Materials/Device structures	PCE (%)	Light intensity	Reference
2001	S. E. Shaheen	MDMO-PPV : PC <sub>61</sub> BM	2.5%	80 mW/cm <sup>2</sup> 27 mW/cm <sup>2</sup>	37
2003	F. Padinger	P3HT : PC <sub>61</sub> BM	3.5%	80 mW/cm <sup>2</sup>	31
2005	Y. Kim	P3HT : PC <sub>61</sub> BM	3.0%	100 mW/cm <sup>2</sup>	32
2005	G. Li	P3HT : PC <sub>61</sub> BM	4.0%	100 mW/cm <sup>2</sup>	33
2005	G. Li	P3HT : PC <sub>61</sub> BM	4.4%	100 mW/cm <sup>2</sup>	34
2005	W. Ma	P3HT : PC <sub>61</sub> BM	5.0%	80 mW/cm <sup>2</sup>	35
2006	Y. Kim	P3HT : PC <sub>61</sub> BM	4.4%	85 mW/cm <sup>2</sup>	36
2007	J. Y. Kim	PCPDTBT : PC <sub>61</sub> BM, P3HT : PC <sub>71</sub> BM (Tandem)	6.5%	100 mW/cm <sup>2</sup>	58
2007	J. Peet	PCPDTBT : PC <sub>71</sub> BM	5.5%	100 mW/cm <sup>2</sup>	47
2009	S. H. Park	PCDTBT : PC <sub>71</sub> BM	6.1%	100 mW/cm <sup>2</sup>	48
2010	Y. Liang	PTB7 : PC <sub>71</sub> BM	7.4%	100 mW/cm <sup>2</sup>	39
2009	H. Chen	PBDTTT-CF : PC <sub>71</sub> BM	7.73%	100 mW/cm <sup>2</sup>	49
2011	S. C. Price	PBnDT-FTAZ : PC <sub>61</sub> BM	7.1%	100 mW/cm <sup>2</sup>	50
2012	Z. He	PTB7 : PC <sub>71</sub> BM (Inverted)	9.2%	100 mW/cm <sup>2</sup>	40
2012	J. S. Moon	PCDTBT : PC <sub>71</sub> BM	6.9%	100 mW/cm <sup>2</sup>	51
2013	W. Li	DT-PDPP2T-TT : PC <sub>71</sub> BM	6.9%	100 mW/cm <sup>2</sup>	52
2013	M. Zhang	PBDTP-DTBT : PC <sub>71</sub> BM	8.07%	100 mW/cm <sup>2</sup>	53
2012	L. Dou	P3HT : ICBA, PBDTT-DPP : PC <sub>71</sub> BM (Tandem)	8.62%	100 mW/cm <sup>2</sup>	59
2013	W. Li	PCDTBT : PC <sub>71</sub> BM, PMDPP3T : PC <sub>61</sub> BM, PMDPP3T : PC <sub>61</sub> BM (Triple Junction)	9.64%	100 mW/cm <sup>2</sup>	60
2013	S. H. Liao	ZnO-C <sub>60</sub> /PTB7-Th : PC <sub>71</sub> BM (Inverted)	9.35%	100 mW/cm <sup>2</sup>	54
2013	X. Guo	PBTI3T : PC <sub>71</sub> BM in CF+DIO (Inverted)	8.46%	100 mW/cm <sup>2</sup>	55
			(Highest FF record >75%)		
2013	J. You	P3HT : ICBA/PDTP-DFBT : PC <sub>61</sub> BM (Tandem)	10.6%	100 mW/cm <sup>2</sup>	61
2014	S. Woo	ZnO/PEI/PTB7 : PC <sub>71</sub> BM (Inverted)	9.2%	100 mW/cm <sup>2</sup>	41

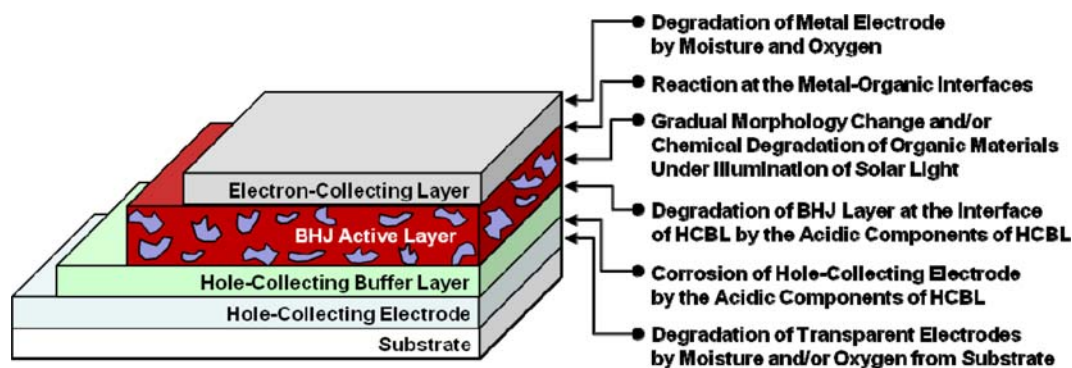


**Fig. 12. Illustration of major issues affecting the stability and lifetime of organic solar cells with bulk heterojunction active layers.**

**Table 3. Summary of key materials/structures used in organic solar cells with all-polymer (polymer : polymer) bulk heterojunction layers**

Year	First author	Materials/Device structures	PCE (%)	Light intensity	Reference
1995	J. J. M. Halls	MEH-PPV : C6-CN-PPV	$V_{oc}=0.6$ V EQE=6%	550 nm, 0.15 mW/cm <sup>2</sup>	19
1995	G. Yu	MEH-PPV : MEH-CN-PPV	0.25-0.9 (EQE=1-6%)	430 nm, 20 mW/cm <sup>2</sup> ~ 1 $\mu$ W/cm <sup>2</sup>	20
1998	M. Granström	POPT/MEH-CN-PPV (19 : 1)/MEH-CN-PPV : POPT (19 : 1) (Laminated double layer)	1.9%	77 mW/cm <sup>2</sup>	69
2001	A. C. Arias	PFB : F8BT	EQE=2-4%	at 3.2 eV	70
2004	Y. Kim	P3HT : F8BT	0.13%	100 mW/cm <sup>2</sup>	71
2004	M. M. Alam	PPV/BBL	1.5%	80 mW/cm <sup>2</sup>	72
2005	T. Kietzke	M3EH-PPV : CN-ether-PPV	1.7%	100 mW/cm <sup>2</sup>	73
2007	C. R. McNeill	P3HT : F8TBT	1.8%	100 mW/cm <sup>2</sup>	74
2007	X. Zhan	BTVP12-PT6 : P(PDI2DD-DTT)	>1% (1.5%)	100 mW/cm <sup>2</sup>	75
2008	Z. Tan	TTV4-PT6 : P(PDI2DD-DTT2)	1.48%	100 mW/cm <sup>2</sup>	76
2009	T. W. Holcombe	POPT/MEH-CN-PPV	2%	100 mW/cm <sup>2</sup>	77
2009	J. A. Mikroyannidis	PPHT : P(PDI-PEPEP)	2.3%	30 mW/cm <sup>2</sup>	78
2010	X. He	P3HT/F8TBT (20 nm planar patterned)	1.85%	100 mW/cm <sup>2</sup>	79
2011	D. Mori	P3HT : PF12TBT	2.0%	100 mW/cm <sup>2</sup>	80
2011	S. Nam	P3HT : F8BT-EBSA (6 : 4)	0.3%	100 mW/cm <sup>2</sup>	81
2011	E. Zhou	PT1 : PC-PDI	2.23%	100 mW/cm <sup>2</sup>	82
2011	J. R. Moore	P3HT : P(NDI2OD-T2)	0.21%	100 mW/cm <sup>2</sup>	83
2012	S. Nam	P3HT-EBSA : F8BT-EBSA	0.4%	100 mW/cm <sup>2</sup>	84
2012	D. Mori	P3HT : PF12TBT	2.7%	100 mW/cm <sup>2</sup>	85
2012	X. Liu	P3HT : PCPDTBT (with BrAni additive)	1.33%	100 mW/cm <sup>2</sup>	86
2012	A. Facchetti group	-	5.2% (NREL)	100 mW/cm <sup>2</sup>	87
2012	M. Schubert	P3HT : P(NDI-TCPDPT) P3HT : P(NDI2OD-T2)	1.1%, 1.4%	100 mW/cm <sup>2</sup>	88
2012	K. Nakabayashi	P3HT : P3HT-PNBI-P3HT	1.28%	100 mW/cm <sup>2</sup>	89
2012	E. Zhou	P3HT : PF-NDI (with DIO additive)	1.63%	100 mW/cm <sup>2</sup>	90
2013	Y. Tang	PTB7 : P(NDI2OD-T2)	1.1%	100 mW/cm <sup>2</sup>	91
2013	N. Zhou	PTB7 : P(NDI2OD-T2)	2.7%	100 mW/cm <sup>2</sup>	92
2013	T. Earmme	PSEHTT : PNDIS-HD/Inverted	3.26%	100 mW/cm <sup>2</sup>	93
2013	A. Facchetti group	-	6.4% (NREL)	100 mW/cm <sup>2</sup>	94

fullerene solar cells is summarized in Table 2. The power conversion efficiency of polymer : fullerene solar cells now passes over ~10% by employing a tandem structure [58-61].

Although the power conversion efficiency of polymer : fullerene solar cells has been improved due to new conjugated polymers and interface control technologies, the stability (lifetime) issue is the most problematic point for polymer : fullerene solar cells. We can separate the stability issue into three sub-categories: (1) degradation of electrodes, (2) chemical degradation of polymers and/or fullerene derivatives, (3) gradual deformation of BHJ morphology (see Fig. 12). As well experienced for commercializing organic light-emitting devices [62], the degradation of metal electrodes can be wisely resolved by hermetic encapsulation to protect from the attack of moisture and/or oxygen. The corrosion of transparent electrode (indium tin oxide - ITO) by the acidic HCBL, for example poly(ethylenedioxythiophene) : poly(styrenesulfonate) (PEDOT : PSS), in the case of normal-type solar cells can be also prevented by controlling the acidity of corresponding solutions and/or by post-treatment processes [63,64]. The chemical degradation of materials requires

new design of molecular structures that are resistant against the attack of singlet oxygen under illumination. However, it is supposed that the gradual deformation of BHJ morphology is not so easy to overcome, even though the glass transition temperatures of both p-type and n-type materials are far higher than typical temperatures upon illumination of solar light [65-68]. Hence a critical study should be concentrated on the stability issue in organic solar cells.

### ALL-POLYMER SOLAR CELLS

In the case of polymer : fullerene solar cells, fullerene derivatives, which are basically classified as one of small molecules though their molecular weight is more than 720, are used as electron acceptors. Hence, strictly speaking, the polymer : fullerene solar cell is not recognized as a perfect plastic solar cell but understood as a polymer composite solar cell. The polymer : fullerene solar cells have an intrinsic limitation because the fullerene derivatives (small molecules) in the polymer : fullerene composite films are vulnerable to migration (or extraction) from one position to another (neighbor-



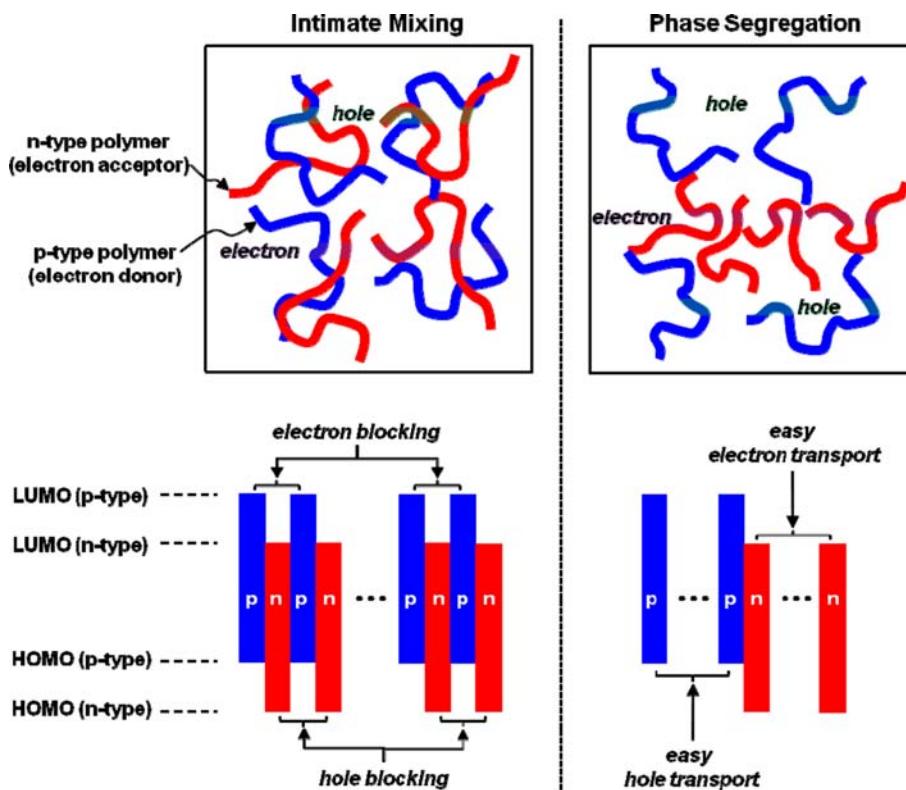


Fig. 13. Importance of forming appropriate charge percolation paths in all-polymer bulk heterojunction films: (left) poor device performance by the presence of huge charge blocking resistances, (b) good device performance by well-organized p-n junctions inside bulk heterojunction films.

ing) position upon bending or rolling so that the stability of resulting flexible solar cells can be poor. To achieve a perfect (flexible) plastic solar cell that can be bendable or rollable, the electron acceptors should be composed of polymers. This type of organic solar cells can be called *polymer : polymer* solar cells or *all-polymer* solar cells. The first all-polymer solar cells were reported in 1995 [19, 20], but their efficiency was quite low and no standard measurement condition was applied. To date, various approaches have been attempted so that the power conversion efficiency of all-polymer solar cells has been increased up to ~3% based on officially published reports [69-93]. We note that ~6.4% efficiency is announced from conference presentations [94]. The reason for the relatively lower efficiency in all-polymer solar cells, compared to polymer : fullerene solar cells, has been suggested as huge charge blocking resistances caused by the intimate mixing of p-type and n-type polymers [71]. As shown in Fig. 13(left), when the p-type and n-type polymers are mixed intimately, each counter (p-type versus n-type) chain acts as a charge blocker leading to poor charge transport efficiency. However, if both p-type and n-type polymers can make an optimum phase segregation state, the charge blocking resistance is expected to be minimized so that the charge transport will not be a crucial limiting factor in achieving high efficiency.

#### FUTURE OUTLOOK

Organic solar cells, whether they are made with small molecules or polymers, have been a challenging research target because of

their potential for next generation solar cells. Although the power conversion efficiency of organic solar cells has been impressively enhanced for such a relatively shorter period, it is thought that a challenging race is yet to come forward for commercialization of organic solar cells. The priority should be on understanding the stability and lifetime of organic solar cells, even though new organic semiconductors such as conjugated polymers should be developed at the same time for breaking new efficiency records. Another effort is also necessary to develop new device structures, which should be more suitable for organic solar cells than for conventional inorganic solar cells. In terms of fabrication technology, a variety of coating processes including slot-die coating method have been tried so far but they should be standardized for individual layers. Finally, it should be stressed that synthesis of well-defined and high purity organic semiconductors is of utmost importance to maintain a commercial level solar cell. For example, chemists and chemical engineers need to concentrate on the technology of large-scale synthesis for achieving high-purity conjugated polymers with narrow polydispersity index and constant molecular weights. Further detailed information on a focused category of polymer-based solar cells can be found in previous reviews [95-99].

#### ACKNOWLEDGEMENTS

This work was financially supported by Korean Government grants (Basic Research Laboratory Program\_2011-0020264, Pioneer Research Center Program\_2012-0001262, Basic Science Research



Program\_2009-0093819, NRF\_2012K1A3A1A09027883, NRF\_2012R1A1B3000523).

## REFERENCES

1. J. Kalowekamo and E. Baker, *Sol. Energy*, **83**, 1224 (2009).
2. A. M. Borchers, J. M. Duke and G. R. Parsons, *Energy Policy*, **35**, 3327 (2007).
3. S. E. Habas, H. A. S. Platt, M. F. A. M. van Hest and D. S. Ginley, *Chem. Rev.*, **110**, 6571 (2010).
4. R. B. Bergmann, *Appl. Phys. A*, **69**, 187 (1999).
5. B. Li, L. Wang, B. Kang, P. Wang and Y. Qiu, *Sol. Energy Mater. Sol. Cells*, **90**, 549 (2006).
6. A. Pochettino, *Acad. Lincei Rend.*, **15**, 355 (1906).
7. J. Koenigsberger, *Ann. Phys.*, **32**, 179 (1910).
8. H. Mette and H. Pick, *Z. Physik*, **134**, 566 (1953).
9. H. Hoegel, *J. Phys. Chem.*, **69**, 755 (1965).
10. H. Kallmann and M. Pope, *J. Chem. Phys.*, **30**, 585 (1959).
11. O. H. LeBlanc Jr., *J. Chem. Phys.*, **30**, 1443 (1959).
12. R. G. Kepler, *Phys. Rev.*, **119**, 1226 (1960).
13. P. Mark and W. Helfrich, *J. Appl. Phys.*, **33**, 205 (1962).
14. N. Geacintov, M. Pope and H. Kallmann, *J. Chem. Phys.*, **45**, 2639 (1966).
15. C. W. Tang, *Appl. Phys. Lett.*, **48**, 183 (1986).
16. B. A. Gregg, M. A. Fox and A. J. Bard, *MRS Proceedings*, 173 (1989).
17. N. S. Sariciftci, L. Smilowitz, A. J. Heeger and F. Wudl, *Science*, **258**, 1474 (1992).
18. G. Yu, J. Gao, J. C. Hummelen, F. Wudl and A. J. Heeger, *Science*, **270**, 1789 (1995).
19. J. J. M. Halls, C. A. Walsh, N. C. Greenham, E. A. Marseglia, R. H. Friend, S. C. Moratti and A. B. Holmes, *Nature*, **376**, 498 (1995).
20. G. Yu and A. J. Heeger, *J. Appl. Phys.*, **78**, 4510 (1995).
21. B. Johnson, M. J. Kendrick and O. Ostroverkhova, *J. Appl. Phys.*, **114**, 094508 (2013).
22. L. Dou, J. You, Z. Hong, Z. Xu, G. Li, R. A. Street and Y. Yang, *Adv. Mater.*, **25**, 6642 (2013).
23. V. Coropceanu, J. Cornil, D. A. da Silva Filho, Y. Olivier, R. Silbey and J.-L. Brédas, *Chem. Rev.*, **107**, 926 (2007).
24. A. Troisi and G. Orlandi, *Phys. Rev. Lett.*, **96**, 086601 (2006).
25. G. Dennler, M. C. Scharber and C. J. Brabec, *Adv. Mater.*, **21**, 1323 (2009).
26. S.-Shajing. Sun and N. Sariciftci, *Organic Photovoltaics*, CRC Press (2005).
27. M. Hiramoto, M. Suezaki and M. Yokoyama, *Chem. Lett.*, **19**, 327 (1990).
28. T. Ameri, G. Dennler, C. Lungenschmied and C. J. Brabec, *Energy Environ. Sci.*, **2**, 347 (2009).
29. C. J. Brabec and J. R. Durrant, *MRS Bull.*, **33**, 670 (2008).
30. F. C. Krebs, *Sol. Energy Mater. Sol. Cells*, **93**, 394 (2009).
31. F. Padinger, R. S. Rittberger and N. S. Sariciftci, *Adv. Funct. Mater.*, **13**, 85 (2003).
32. Y. Kim, S. A. Choulis, J. Nelson, D. D. C. Bradley, S. Cook and J. R. Durrant, *Appl. Phys. Lett.*, **86**, 063502 (2005).
33. G. Li, V. Shrotriya, Y. Yao and Y. Yang, *J. Appl. Phys.*, **98**, 043704 (2005).
34. G. Li, V. Shrotriya, J. Huang, Y. Yao, T. Mariarty, K. Emery and Y. Yang, *Nat. Mater.*, **4**, 864 (2005).
35. W. L. Ma, C. Y. Yang, X. Gong, K. Lee and A. J. Heeger, *Adv. Funct. Mater.*, **15**, 1617 (2005).
36. Y. Kim, S. Cook, S. M. Tuladhar, S. A. Choulis, J. Nelson, J. R. Durrant, D. D. C. Bradley, M. Giles, I. McCulloch, C.-S. Ha and M. Ree, *Nat. Mater.*, **5**, 197 (2006).
37. S. E. Shaheen, C. J. Brabec and N. S. Sariciftci, *Appl. Phys. Lett.*, **78**, 841 (2001).
38. H. Hoppe, T. Glatzel, M. Niggemann, W. Schwinger, F. Schaeffler, A. Hinsch, M. Ch. Lux-Steiner and N. S. Sariciftci, *Thin Solid Films*, **511-512**, 587 (2006).
39. Y. Y. Liang, Z. Xu, J. B. Xia, S.-T. Tsai, Y. Wu, G. Li, C. Ray and L. P. Yu, *Adv. Mater.*, **22**, E135 (2010).
40. Z. C. He, C. M. Zhong, S. J. Su, M. Xu, H. B. Wu and Y. Cao, *Nat. Photonics*, **6**, 591 (2012).
41. S. Woo, W. H. Kim, H. Kim, Y. Yi, H.-K. Lyu and Y. Kim, *Adv. Energy Mater.*, **4**, 1301692 (2014).
42. X. Yang, J. K. J. van Duren, R. A. J. Janssen, M. A. J. Michels and J. Loos, *Macromolecules*, **37**, 2151 (2004).
43. Y. Kim, S. Cook, S. A. Choulis, J. Nelson, J. R. Durrant and D. D. C. Bradley, *Proceedings of IEEE 3<sup>rd</sup> World Conference on Photovoltaic Energy Conversion*, 1LN-C-01 (2004) (presented in 2002).
44. Y. Kim, S. Cook, S. A. Choulis, J. Nelson, J. R. Durrant and D. D. C. Bradley, Presented in the *International Conference on Physics, Chemistry and Engineering of Solar Cells*, Spain (2004).
45. Y. Kim, M. Shin, H. Kim, Y. Ha and C.-S. Ha, *J. Phys. D: Appl. Phys.*, **41**, 225101 (2008).
46. Y. He, H.-Y. Chen, J. Hou and Y. Li, *J. Am. Chem. Soc.*, **132**, 1377 (2010).
47. J. Peet, J. Y. Kim, N. E. Coates, W. L. Ma, D. Moses, A. J. Heeger and G. C. Bazan, *Nat. Mater.*, **6**, 497 (2007).
48. S. H. Park, A. Roy, S. Beaupre, S. Cho, N. E. Coates, J. S. Moon, D. Moses, M. Leclerc, K. Lee and A. J. Heeger, *Nat. Photon.*, **3**, 297 (2009).
49. H. Chen, J. Hou, S. Zhang, Y. Liang, G. Yang, Y. Yang, L. Yu, Y. Wu and G. Li, *Nat. Photon.*, **3**, 649 (2009).
50. S. C. Price, A. C. Stuart, L. Yang, H. Zhou and W. You, *J. Am. Chem. Soc.*, **133**, 4625 (2011).
51. J. S. Moon, J. Jo and A. J. Heeger, *Adv. Energy Mater.*, **2**, 304 (2012).
52. W. Li, K. H. Hendriks, W. S. C. Roelofs, Y. Kim, M. M. Wienk and R. A. J. Janssen, *Adv. Mater.*, **25**, 3182 (2013).
53. M. Zhang, Y. Gu, X. Guo, F. Liu, S. Zhang, L. Huo, T. P. Russell and J. Hou, *Adv. Mater.*, **25**, 4944 (2013).
54. S. H. Liao, H. J. Jhuo, Y. S. Cheng and S. A. Chen, *Adv. Mater.*, **25**, 4766 (2013).
55. X. Guo, N. Zhou, S. J. Lou, J. Smith, D. B. Tice, J. W. Hennek, R. P. Ortiz, J. T. L. Navarrete, S. Li, J. Strzalka, L. X. Chen, R. P. H. Chang, A. Facchetti and T. J. Marks, *Nat. Photon.*, **7**, 825 (2013).
56. S. Cook, A. Furube, R. Katoh and L. Han, *Chem. Phys. Lett.*, **478**, 33 (2009).
57. A. Nogimura, K. Akaike, R. Nakanishi, R. Eguchi and K. Kanai, *Org. Electron.*, **14**, 3222 (2013).
58. J. Y. Kim, K. Lee, N. E. Coates, D. Moses, T.-Q. Nguyen, M. Dante and A. J. Heeger, *Science*, **317**, 222 (2007).
59. L. T. Dou, J. B. You, J. Yang, C.-C. Chen, Y. J. He, S. Murase, T. Moriarty, K. Emery, G. Li and Y. Yang, *Nat. Photon.*, **6**, 180 (2012).
60. W. Li, A. Furlan, K. H. Hendriks, M. M. Wienk and R. A. J. Jans-

- sen, *J. Am. Chem. Soc.*, **135**, 5529 (2013).
61. J. B. You, L. T. Dou, K. Yoshimura, T. Kato, K. Ohya, T. Moriarty, K. Emery, C. C. Chen, J. Gao, G. Li and Y. Yang, *Nat. Commun.*, **4**, 1446 (2013).
  62. Y. Kim and C. S. Ha, *Advances in Organic Light-Emitting Devices*, Trans Tech Publications, Zürich (2008).
  63. H. Kim, S. Nam, H. Lee, S. Woo, C. S. Ha, M. Ree and Y. Kim, *J. Phys. Chem. C*, **115**, 13502 (2011).
  64. S. Lee, S. Nam, H. Lee, H. Kim and Y. Kim, *ChemSusChem*, **4**, 1607 (2011).
  65. H. Kim, M. Shin, J. Park and Y. Kim, *ChemSusChem*, **3**, 476 (2010).
  66. J. A. Hauch, P. Schilinsky, S. A. Choulis, R. Childers, M. Biele and C. J. Brabec, *Sol. Energy Mater. Sol. Cells*, **92**, 727 (2008).
  67. F. C. Krebs, J. E. Carlé, N. C. Bagger, M. Andersen, M. R. Lilliedal, M. A. Hammond and S. Hvidt, *Sol. Energy Mater. Sol. Cells*, **86**, 499 (2005).
  68. S. Schuller, P. Schilinsky, J. Hauch and C. J. Brabec, *Appl. Phys. A-Mater.*, **79**, 37 (2004).
  69. M. Granström, K. Petritsch, A. C. Arias, A. Lux, M. R. Andersson and R. H. Friend, *Nature*, **395**, 257 (1998).
  70. A. C. Arias, J. D. MacKenzie, R. Stevenson, J. J. M. Halls, M. Inbasekaran, E. P. Woo, D. Richards and R. H. Friend, *Macromolecules*, **34**, 6005 (2001).
  71. Y. Kim, S. Cook, S. A. Choulis, J. Nelson, J. R. Durrant and D. D. C. Bradley, *Chem. Mater.*, **16**, 4812 (2004).
  72. M. M. Alam and S. A. Jenekhe, *Chem. Mater.*, **16**, 4647 (2004).
  73. T. Kietzke, H. H. Hróhold and D. Neher, *Chem. Mater.*, **17**, 6532 (2005).
  74. C. R. McNeill, A. Abruci, J. Zaumseil, R. Wilson, M. J. McKiernan, J. H. Burroughes, J. J. M. Halls, N. C. Greenham and R. H. Friend, *Appl. Phys. Lett.*, **90**, 193506 (2007).
  75. X. Zhan, Z. Tan, B. Domercq, Z. An, X. Zhang, S. Barlow, Y. Li, D. Zhu, B. Kippelen and S. R. Marder, *J. Am. Chem. Soc.*, **129**, 7246 (2007).
  76. Z. A. Tan, E. J. Zhou, X. W. Zhan, X. Wang, Y. F. Li, S. Barlow and S. R. Marder, *Appl. Phys. Lett.*, **93**, 073309 (2008).
  77. T. W. Holcombe, C. H. Woo, D. F. J. Kavulak, B. C. Thompson and J. M. J. Fréchet, *J. Am. Soc. Chem.*, **131**, 14160 (2009).
  78. J. A. Mikroyannidis, M. M. Stylianakis, G. D. Sharma, P. Balraju and M. S. Roy, *J. Phys. Chem. C*, **113**, 7904 (2009).
  79. X. He, F. Gao, G. Tu, D. Hasko, S. Hüttner, U. Steiner, N. C. Greenham, R. H. Friend and W. T. S. Huck, *Nano Lett.*, **10**, 1302 (2010).
  80. D. Mori, H. Bente, J. Kosaka, H. Ohkita, S. Ito and K. Miyake, *ACS Appl. Mater. Interfaces*, **3**, 2924 (2011).
  81. S. Nam, M. Shin, H. Kim, C. S. Ha, M. Ree and Y. Kim, *Adv. Funct. Mater.*, **21**, 4527 (2011).
  82. E. Zhou, J. Cong, Q. Wei, K. Tajima, C. Yang and K. Hashimoto, *Angew. Chem. Int. Ed.*, **50**, 2799 (2011).
  83. J. R. Moore, S. A. Seifried, A. Rao, S. Massip, B. Watts, D. J. Morgan, R. H. Friend, C. R. McNeill and H. Sirringhaus, *Adv. Energy Mater.*, **1**, 230 (2011).
  84. S. Nam, M. Shin, S. Park, S. Lee, H. Kim and Y. Kim, *Phys. Chem. Chem. Phys.*, **14**, 15046 (2012).
  85. D. Mori, H. Bente, H. Ohkita, S. Ito and K. Miyake, *ACS Appl. Mater. Interfaces*, **4**, 3325 (2012).
  86. X. Liu, S. Huettner, Z. Rong, M. Sommer and R. H. Friend, *Adv. Mater.*, **24**, 669 (2012).
  87. A. Facchetti, *Presented at the 3<sup>rd</sup> Conference on Organic Photovoltaics*, Würzburg, Germany (2012), <http://faculty.wcas.northwestern.edu/~afa912/>.
  88. M. Schubert, D. Döf, J. Frisch, S. Roland, R. Steyrleuthner, B. Stiller, Z. Chen, U. Scherf, N. Koch, A. Facchetti and D. Neher, *Adv. Energy Mater.*, **2**, 369 (2012).
  89. K. Nakabayashi and H. Mori, *Macromolecules*, **45**, 9618 (2012).
  90. E. Zhou, J. Cong, M. Zhao, L. Zhang, K. Hashimoto and K. Tajima, *Chem. Commun.*, **48**, 5283 (2012).
  91. Y. Tang and C. R. McNeill, *J. Polym. Sci. Part B: Polym. Phys.*, **51**, 403 (2013).
  92. N. Zhou, H. Lin, S. J. Lou, X. Yu, P. Guo, E. F. Manley, S. Loser, P. Hartnett, H. Huang, M. R. Wasielewski, L. X. Chen, R. P. H. Chang, A. Facchetti and T. J. Marks, *Adv. Energy Mater.* (2013), DOI: 10.1002/aenm.201300785.
  93. T. Earmme, Y. J. Hwang, N. M. Murari, S. Subramaniyan and S. A. Jenekhe, *J. Am. Chem. Soc.*, **135**, 14960 (2013).
  94. A. Facchetti, *Presented at the Hybrid and Organic Photovoltaic Conference*, Sevilla, Spain (2013), <http://faculty.wcas.northwestern.edu/~afa912/>.
  95. J. Nelson, *Mater. Today*, **14**, 462 (2011).
  96. G. Dennler, M. C. Scharber and C. J. Brabec, *Adv. Mater.*, **21**, 1323 (2009).
  97. P. W. M. Blom, V. D. Mihailescu, L. J. A. Koster and D. E. Markov, *Adv. Mater.*, **19**, 1551 (2007).
  98. A. C. Mayer, S. R. Scully, B. E. Hardin, M. W. Rowell and M. D. McGehee, *Mater. Today*, **10**, 28 (2007).
  99. G. Li, R. Zhu and Y. Yang, *Nat. Photon.*, **6**, 153 (2012).



**Youngkyoo Kim** received B.S., M.S. and Ph.D degrees in *Engineering* from the department of polymer science and engineering, Pusan National University in 1991, 1993 and 1996, and the second Ph.D degree in Physics from the department of physics, Imperial College London in 2006. In 2007 he founded *Organic Nanoelectronics Laboratory* (ONELAB – <http://one.knu.ac.kr>) at the department of chemical engineering, Kyungpook National University (Republic of Korea). He has various professional experiences with the Institute for Advanced Engineering (IAE) and LG Innotek for OLEDs and future technology, while he has been a technical consultant for Samsung Display and medium-size companies for OLED and LCD materials and devices. His research interest includes organic electronic materials and devices, artificial sensory devices (skins), olfactory devices, biomedical devices, ultrafast optoelectronics.